CHEMISTRY & CHEMICAL TECHNOLOGY

Chem. Chem. Technol., 2022,
Vol. 16, No. 3, pp. 345–358

Chemistry

SELECTIVE REMOVAL OF MERCURY(II) USING HYDROGELS PREPARED BY GAMMA RADIATION

Dursun Saraydın[1, ✉], Ebru Şahin Yıldırım[2], Erdener Karadağ[3]

https://doi.org/10.23939/chcht16.03.345

Abstract. To selectively remove mercury(II), 2-hydroxyethyl methacrylate (HM) and 2-hydroxyethyl methacrylate/acrylamide (HM/ACR) hydrogels were synthesized using radiation. These hydrogels were used in swelling, diffusion, and binding studies. Swelling parameters for HM/ACR−Hg^{2+} system are higher than those of HM−Hg^{2+} systems. Binding of Hg^{2+} has been observed to be C-type for HM and L-type for HM/ACR hydrogels. Binding parameters were calculated using Freundlich, Langmuir and Henry models. Effects of Hg^{2+} concentration, radiation dose, ACR ratio, temperature, counter ions were investigated. Binding and swelling of HM increased with the incorporation of acrylamide. HM/ACR hydrogels absorbed only Hg^{2+}, and did not absorb heavy metal ions.

Keywords: mercury, 2-hydroxyethyl methacrylate, acrylamide, hydrogel, radiation, adsorption.

1. Introduction

Mercury, which ranks third among the 275 toxic substances listed by the Toxic Substances and Disease Records Substance Priority List[1] in 2019, is a chemical element that exists throughout the environment. Mercury, which can be transported to the atmosphere,[2,3] stays in the environment for a long time and accumulates in the food network, causing various health problems due to its toxic properties.[4,5] Despite this disadvantage, mercury has been used in many areas and is still used for many different purposes.[2]

Mercury can be present as HgO, inorganic (Hg^{+} and Hg^{2+}), and organic (*i.e.*, MeHg, EtHg, and PhHg). Hg^{2+} is the predominant form of mercury in water and soil or sediment. All forms of mercury are highly toxic to all organisms. It can easily penetrate through the cell membrane and accumulate in the blood.[6-9]

It has been proposed that adsorbents can be used to remove and concentrate metals from industrial wastewaters. Adsorbents made of polymers are widely used in heavy metal removal from aqueous systems due to their selectivity and efficiency, easiness of use, and low price.[10-12] However, hydrogels, polymeric network structures, have been used to remove Hg^{2+} in a limited number.[13-16]

Hydrogels are crosslinked, three-dimensional hydrophilic polymer networks which show kaleidoscopic swelling because of inherent crosslinks. Water-loving functional groups, *i.e.*, hydroxyl, carboxylic, amidic, sulfonyl, *etc*., which may be present in the hydrogel, absorb water, thereby enhancing the hydrogel ability to retain water.

One can perform the synthesis of the hydrogel by crosslinking hydrophilic monomers. The crosslinking reaction may be carried out either by chemical crosslinking agents or by radiation. In radiation processing technology there is no need for initiators, catalysts and crosslinkers for the hydrogel synthesis due to the high energy of ionizing radiations.[17-19] The radiation crosslinking technique has numerous advantages. Radiation technology is environmentally friendly as it does not leave residues or contaminants in the environment.[20]

When hydrogels interact with dissolved substances in a solution, they adsorb and retain them. Therefore, hydrogels have been used in many investigations, such as for water purification, for removal of some water-soluble dyes or toxic metal ions from aqueous solutions.[13]

Due to the growing awareness of environmental mercury pollution and the need for new and selective methods for the removal of Hg^{2+} from natural water or wastewaters, this research is devoted to the design, preparation and application of radiation crosslinked 2-hydroxyethyl methacrylate (HM) homopolymer and 2-hydroxyethyl methacrylate/acrylamide (HM/ACR) copolymer as selective for Hg^{2+}.

The goal of this research is to investigate the potential of HM and HM/ACR hydrogels to selectively adsorb Hg^{2+} ions from the individual artificial aqueous solution. Firstly, HM and HM/ACR hydrogels were

[1] Sivas Cumhuriyet University, Science Faculty, Chemistry Department, Sivas, Turkey
[2] Sivas Cumhuriyet University, Imranlı Vocational School, Imranlı, Sivas, Turkey
[3] Adnan Menderes University, Science & Letter Faculty Chemistry Department, Aydın, Turkey
✉ *saraydin@cumhuriyet.edu.tr; dsaraydin@gmail.com*

prepared; secondly, the effect of interaction time, initial concentration of Hg^{2+} solutions, radiation dose, monomer:comonomer ratio, counterions, and temperature on the removal ability of HM and HM/ACR hydrogels were investigated. Freundlich and Langmuir or Henry isotherm models are used to defining equilibrium data. Finally, the removal mechanisms of Hg^{2+} from the artificial aqueous solution on HM and HM/ACR hydrogels were also evaluated in terms of thermodynamics, and the desorption efficiency was also investigated.

2. Experimental

2.1. Chemicals

2-Hydroxymethyl methacrylate (HM) and acrylamide (ACR) are produced by BDH (Poole, UK). $Hg(OOCCH_3)_2$, $Hg(NO_3)_2$, $HgSO_4$, $HgCl_2$, $Cu(OOCCH_3)_2$, $Pb(OOCCH_3)_2$, $Zn(OOCCH_3)_2$, $Cd(OOCCH_3)_2$, and 1,5-diphenyl carbazide were purchased from Merck (Darmstadt, Germany). All chemicals were used as received.

2.2. Preparation of Hydrogels

10 mL of HM with 0, 2, 4, 6, 8, or 10 g of ACR were dissolved in 10, 12, 14, 16, 18, and 20 mL of double distilled water, respectively. These solutions were filled into PVC pipettes using a syringe. Doses of 2, 3, 4, 5, and 6 kGy in a Gammacell 220 type γ-irradiator were applied at a fixed rate of 6 $kGy \cdot h^{-1}$. Cylindrical hydrogels were cut, kept in double distilled water to remove unreacted monomers, dried in ambient air, and then in a vacuum.[21]

Unless otherwise indicated, HM or HM/ACR hydrogels containing 5 g ACR were used in the swelling and binding experiments. All experiments were carried out at 283 K for 8 h and at the original solution pH, to get rid of buffer ions.

2.3. Hydrogels Analysis

Swelling of hydrogels. HM and HM/ACR hydrogels irradiated to 2 kGy were swelled at 283 K in water and mercury(II) acetate solution (100 $mg \cdot L^{-1}$). The mass of the swollen gels was determined by weighing at certain time intervals.

The swelling (S) can be given as following equation:

$$S = \frac{m_w}{m_0} \quad (1)$$

where m_0 and m_w are the initial mass of gel and the mass of water in the hydrogel (g) at any time, respectively.[21]

Spectroscopic analysis. Homopolymerization of HM, copolymerization of HM/ACR, and Hg^{2+}-hydrogel interactions were verified using the MATTSON 1000 FTIR spectrometer.

Adsorption kinetics. For adsorption kinetics, four kGy irradiated HM or HM/ACR hydrogels were added to the $Hg(OOCCH_3)_2$ solution (100 $mg \cdot L^{-1}$) and the concentration of Hg^{2+} in the remaining solution was determined at appropriate intervals.

Adsorption equilibrium. 5 kGy irradiated HM or HM/ACR hydrogel was placed to 20 mL of $Hg(OOCCH_3)_2$ solution with concentrations of 10–250 $mg \cdot L^{-1}$ and kept for 8 h.

Effect of ACR ratio in hydrogel and Irradiation dose on adsorption. Hydrogels synthesized at various ACR ratios and irradiation doses were allowed to equilibrate by placing them in a 20 mL of $Hg(OOCCH_3)_2$ solution (100 $mg \cdot L^{-1}$).

Effect of temperature. 2 kGy irradiated HM or HM/ACR hydrogels were allowed to equilibrate at temperatures of 283–323 K by transferring them to 50 mL of $Hg(OOCCH_3)_2$ solution (100 $mg \cdot L^{-1}$).

Effect of counterions. 4 kGy irradiated HM or HM/ACR hydrogels were added to 50 mL of mercury salt solutions containing CH_3COO^- or NO_3^- or SO_4^{2-} or Cl^- ions (100 $mg \cdot L^{-1}$) and kept until equilibrated.

Determination of Hg^{2+} ions. Mercury ion concentrations were determined by adding 1 mL of 1.5-diphenyl carbazide solution at a concentration of 0.001 $g \cdot L^{-1}$ with 1 ml of distilled water to 1 mL of Hg^{2+} solution.[22] Absorption of purple-colored mercury complexes was measured at a Shimadzu 160 A model UV/VIS spectrophotometer at a wavelength of 530 nm.

Selectivity. Selectivity trials of 3 kGy irradiated HM or HM/ACR hydrogels were carried out by placing 50 mL of acetate salts (*i.e.* mercury, copper, lead, zinc, and cadmium) in a metal solution mixture of 100 $mg \cdot L^{-1}$. Metal concentrations were found with an atomic absorption spectrophotometer (Shimadzu AAS - 6300S model).

Recovery. Hg-loaded hydrogels were boiled in acetic acid for 1 h and cooled; then the absorbance of the complex formed by adding 1.5-diphenyl carbazide solution was measured at 530 nm.

3. Results and Discussion

3.1. Preparation

Hydrogels were synthesized using ionizing ^{60}Co gamma radiation.[17,19] ^{60}Co gamma radiation, which is used in the production of polymers and gels from monomers, and changes the properties of synthetic polymers, provides a clean method. It is unnecessary to add any chemicals such as initiators, catalysts, and

accelerators to the reaction medium. Polymerization is carried out with free radicals generated from a monomer, comonomer, or solvent. Therefore, no residues of chemicals, catalyst, *etc*. remain in the polymeric structure after radiation application.

Free radicals are generated when the HM and/or ACR monomers in aqueous solutions are irradiated with gamma rays. HM homopolymers or HM/ACR copolymers are formed by random reactions of free radicals consisting of water, monomers or comonomers with the monomers in the environment. Gamma irradiation of 2 kGy at room temperature is sufficient for the complete gelling of HM or ACR.[21,23]

3.2. FT-IR Analysis

In the spectrum of the crosslinked HM homopolymer (Fig 1), the weak absorption band at 2876 cm^{-1} corresponds to the C–H stretching vibration of the methylene groups. The sharp band at 1728 cm^{-1} corresponds to the C=O group. The wide O–H stretching absorption band at 3600–3200 cm^{-1} shows the H-bond between hydroxyl groups in HM.

The spectrum of the crosslinked HM/ACR copolymer (Fig 1) shows all characteristic bands of the HM homopolymer. In the spectrum of the copolymer, there are wide absorption bands of hydroxyl (–OH) groups in HM and amide ($–NH_2$) groups in ACR at 3620−3150 cm^{-1}. The absorption bands of the methyl group in HM and the amide group in ACR at 1293 and 1448 cm^{-1} are observed in the spectrum of the HM/ACR hydroge.[24] On the other hand, HM/ACR copolymer shows a characteristic band at 1728 cm^{-1} (C=O stretching, amide I). The bands in the range of 3600–3150 and 1450 cm^{-1} are the stretching vibrations of amide groups.[24]

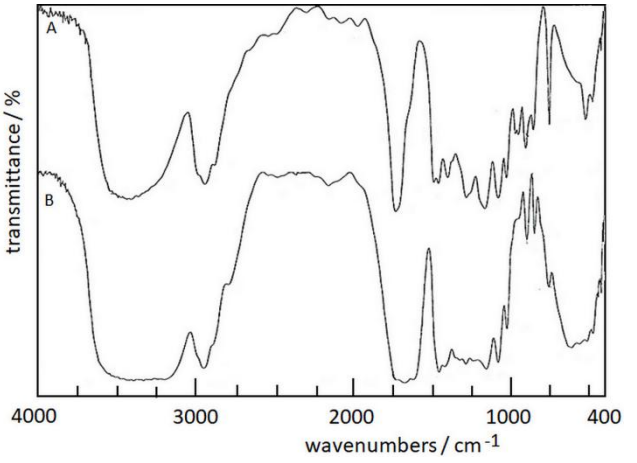

Fig. 1. FTIR spectra of the hydrogels: HM (A) and HM/ACR (B)

C=C olefinic stretching vibrations of monomeric double bonds at 900–1000 and 1516 cm^{-1} are not seen in the spectra of the HM and HM/ACR hydrogels. This clearly shows that monomers and comonomers are homo- and/or co-polymerized.[25] From this spectral analysis, it can be said that a polymer is formed by polymerizing over the double bonds of HM and ACR monomers.

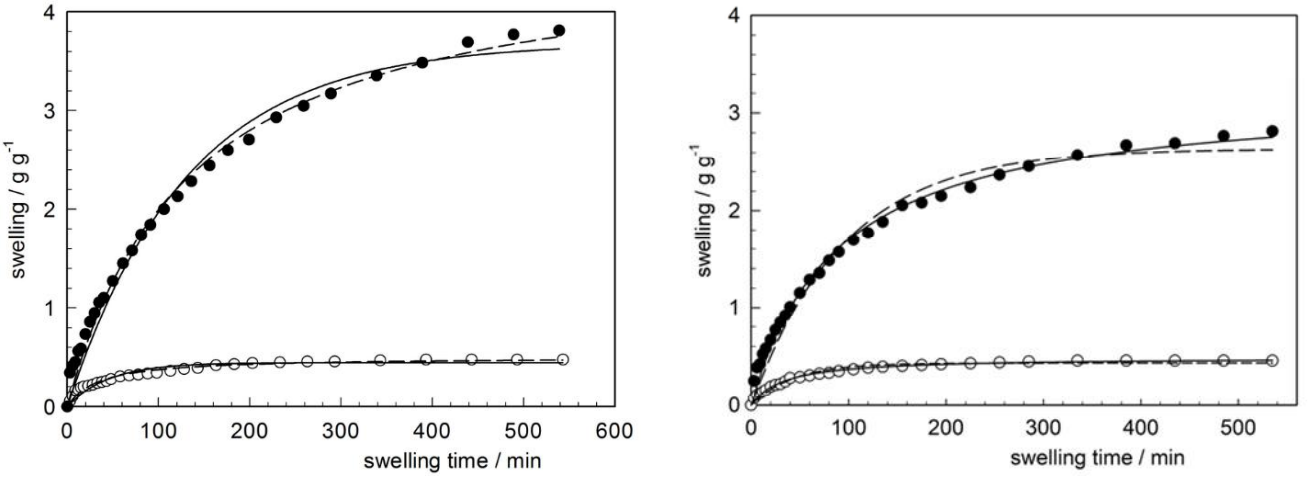

a) b)

Fig. 2. The swelling curves of the hydrogels in distilled water (a) and in the Hg^{2+}solution (b): HM (○); HM/ACR (●);pseudo-first order model fit (− − −) and pseudo-second order model fit (——)

Table 1. Kinetics parameters of the hydrogel swelling

Parameters	Hydrogel			
	HM		HM/ACR	
	in water	in Hg^{2+} solution	in water	in Hg^{2+}solution
Experimental				
Equilibrium swelling, S_{eq}, g g^{-1}	0.4762	0.4561	3.8107	2.8163
Pseudo-first order				
Power parameter S_e, g g^{-1}	0.4434	0.4327	3.6824	2.6385
Rate parameter τ, min	45.45	42.37	129.87	95.34
Swelling rate SR, g g^{-1} min^{-1}	0.0098	0.0102	0.0284	0.0277
Rate constant $k_{1,S}$, min^{-1}	0.0220	0.0236	0.0077	0.0105
Correlation coefficient R^2	0.9622	0.9668	0.9831	0.9774
Pseudo-second order				
Maximum swelling S_e, g g^{-1}	0.4994	0.4882	4.6904	3.2134
Initial rate r_0 , $(dS/dt)_0$, g g^{-1} min^{-1}	0.0148	0.0151	0.0348	0.0362
Rate constant $k_{2,S}$, g g^{-1} min^{-1}	0.0037	0.0035	0.7651	0.3755
Correlation coefficient R^2	0.9745	0.9937	0.9928	0.9926

3.3. Swelling and Diffusion

The swelling of the hydrogels over time is shown in Fig. 2, and the values with constant water intake (equilibrium swelling, S_{eq}) are given in Table 1.

The hydrophilicity of the HM/ACR copolymer containing water-loving groups, such as amine and carbonyl group is higher than that of the homopolymer containing the water-loving hydroxyl and carboxyl group, as well as hydrophobic groups such as the $-(CH_2)_2-$ and methyl group. The more hydrophilic gel will absorb more water, and therefore the HM/ACR copolymer will swell considerably more than the HM hydrogel.

Fig. 2 and Table 1 show that the fast-swelling HM/ACR hydrogel swells by about 6-8 times more than the HM hydrogel. Besides, while HM/ACR hydrogel swells in water by 1.44 times more than Hg^{2+} solution, HM hydrogel swells in water only by 1.04 times more than Hg^{2+} solution.

3.3.1. Swelling kinetics

A wide variety of kinetic models has been proposed to explain the swelling mechanism.[26,27] The pseudo-order kinetics model is given by the following equation:

$$\frac{dS}{dt} = k_{i,s}(S_e - S)^n \quad (2)$$

where $k_{i,S}$ is the rate constant; S and S_e are the swelling at any time and equilibrium, respectively; n indicates the pseudo-order of swelling.

After integration in boundary conditions, Eq. (2) has a following view:

$$\text{for } n = 1 \quad S = S_{\max}(1 - e^{k_{1,s}t}) \quad (3)$$

$$\text{for } n = 2 \quad S = \frac{t}{A + Bt} \quad (4)$$

where A is the term related to the initial swelling rate r_0; B is the term related to equilibrium swelling, *i.e.* $A = 1/k_{2,s} \cdot S_e^2$ and $B = 1/S_e$.[26,27]

S-t plots were drawn using a nonlinear regression (Fig. 2); calculated kinetic parameters and correlation coefficients R^2 are tabulated in Table 1.

For pseudo-first order kinetics (PFO), the ratio of power parameter (S_e) to the rate parameter gives the swelling rate (SR, g g^{-1} min^{-1}) at time τ, while the inverse of the rate parameter gives the rate constant ($k_{1,S}$, min^{-1}). The rate parameter value is a measure of the SR (*i.e.*, the lower the τ value, the higher the rate of swelling).[26] The rate parameters are found to be 42 and 45 min for the HM hydrogels, and 95 and 130 min for the HM/ACR hydrogels, respectively (Table 1). It means that according to the model (Eq. 3), these samples absorb approximately 63 % of their maximum absorption capacity during 42−130 min. These results show that the HM/ACR hydrogel rapidly swollen, and the HM/ACR hydrogels swollen by about 6–8 times more than HM hydrogels. Moreover, while the swelling rate of HM/ACR hydrogel in water was by 1.44 times more than Hg^{2+} ion solution, the values of HM hydrogel in water were by 1.04 times more than Hg^{2+} ions.

The theoretical S_e value found in the pseudo-second order kinetic model (PSO) is very close to the experimental S_{eq} value. So, PSO is an agreement with swelling experiments. The results revealed that the R^2 of the PSO was higher than those of the PFO, indicating that the PSO better represented the swelling of the hydrogels.

3.3.2. Diffusion

The diffusion of fluid into hydrogels is calculated according to Eq. (5):

$$F = k_D t^n \quad (5)$$

where F is the fractional water uptake at time t; k_D is a constant incorporating characteristic of the gel and the fluid; and n is the diffusional exponent, indicative of the transport mechanism.

This equation is valid for the first 60 % of F. It shows Fickian diffusion if $n = 0.5$, non-Fickian diffusion if $0.5 > n > 1$, and Case II transport behavior if $n = 1$.[16,27]

For HM and HM/ACR hydrogels, the F-t plots are drawn (Fig. 3), and n and k_D parameters are calculated using the nonlinear regression. These parameters and correlation coefficients R^2 are given in Table 2.

The value of n is found to be below 0.50 for HM hydrogel, and over 0.50 for HM/ACR hydrogel. While the diffusion of water into the HM hydrogel is of Fickian character, it is of non-Fickian character for the HM/ACR hydrogel.[14]

Diffusion coefficient, D ($cm^2 \cdot s^{-1}$), is calculated according to Eq. (6):

$$D = \left(\frac{k_D}{4}\right)^2 \pi r^2 \qquad (6)$$

where r is the hydrogel radius.[27]

The D values change from $12.5 \cdot 10^{-7}$ to $5.29 \cdot 10^{-7}$ $cm^2\ s^{-1}$ (Table 2), and they are higher in water than those of ions. Therefore diffusion of the big hydrated mercury(II) ions [$Hg(H_2O)_6^{2+}$] into the small hydrogel pores is difficult to be held there.

3.4. Removal of Hg^2 from the Solutions

3.4.1. Binding of Hg^{2+} to HM and HM/ACR hydrogels

Since HM is a neutral polymer, it has not been used directly in the adsorption of metal ions; however, it has been used for metal adsorption by chemical modifications *via* the hydroxyl group[28,29] or by grafting it into some polymer backbones.[30,31] HM chemical modifications and grafts are a complex and very difficult process that takes a long time.

Like HM, ACR is a neutral polymer and does not adsorb any heavy metal ions other than mercury ions. Monoamido or diamido groups in amide compounds react with mercury ions. The mercury-amide linkage is covalent rather than coordinative. Amide groups show a minimum coordination tendency with transition metal ions since they are a weak donor due to the electron-attracting carbonyl group. This feature makes amide groups unique in the highly selective mercury binding.[31,32] Therefore, HM/ACR hydrogels were designed to give HM the ability to absorb mercury. These gels containing amide groups can be used to remove mercury ions. Besides, mercury-loaded adsorbents can be easily regenerated with hot CH_3COOH without hydrolysis of amides.[32]

To investigate the binding of Hg^{2+} to HM and HM/ACR polymers, the hydrogels were placed in aqueous $Hg(OOCCH_3)_2$ solutions and kept for one day until equilibrium. Then, a steep decrease in the concentration of Hg^{2+} is observed. Thus, the incorporation of ACR in HM hydrogels enhanced the interaction between Hg^{2+} and the constitutional repeating units of ACR in the hydrogel network.

The pH value of the original Hg^{2+}solutions used in these binding experiments was measured at approximately 4.5. All binding studies were made at the original pH of the solutions as the optimum pH value because as the pH increases, the formation of hydrogel−Hg^{2+}complexes increases too. At acidic pH values, the excess H^+ ion competes with Hg^{2+} for active sites on hydrogels. As pH rises to 4−5 and proton concentration decrements, this competition decreases and the formation of complexes between hydrogels and Hg^{2+} increases.[29,33]

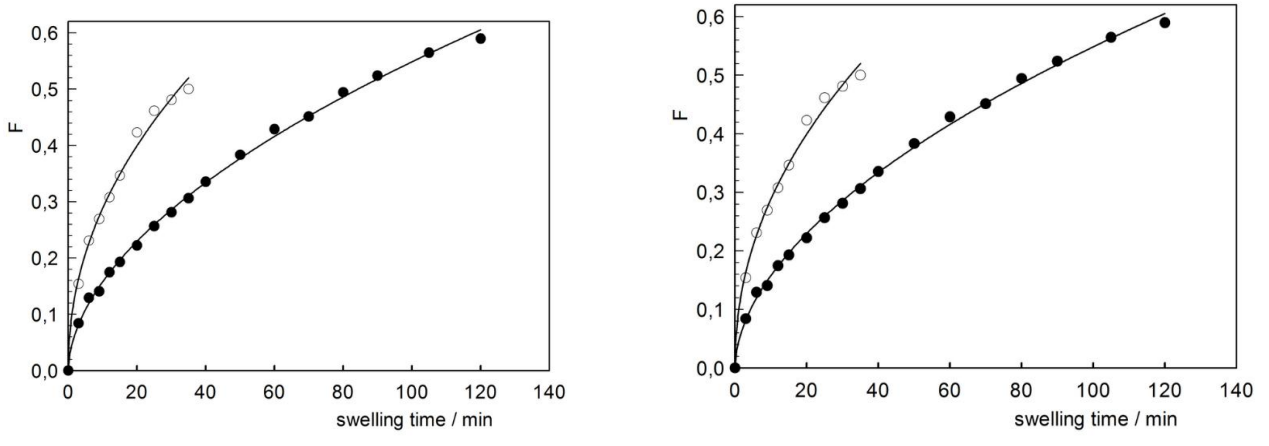

a) b)

Fig. 3. Plots of F *vs.* t of the hydrogels in distilled water (a), and in the Hg^{2+}solution (b): HM (○); HM/ACR (●) and model fit (——)

Table 2. Diffusion parameters of the hydrogels

Parameters	Hydrogel			
	HM		HM/ACR	
	in water	in Hg^{2+} solution	in water	in Hg^{2+} solution
Diffusion constant k_D	0.1201	0.0978	0.0316	0.0454
Diffusion exponent n_D	0.4030	0.4071	0.5712	0.5410
Diffusion mechanism type	Fickian	Fickian	non-Fickian	non-Fickian
Correlation coefficient R^2	0.9683	0.9937	0.9982	0.9984
Diffusion coefficient D, $cm^2 \cdot s^{-1}$	$2.50 \cdot 10^{-6}$	$1.25 \cdot 10^{-6}$	$6.32 \cdot 10^{-7}$	$5.29 \cdot 10^{-7}$

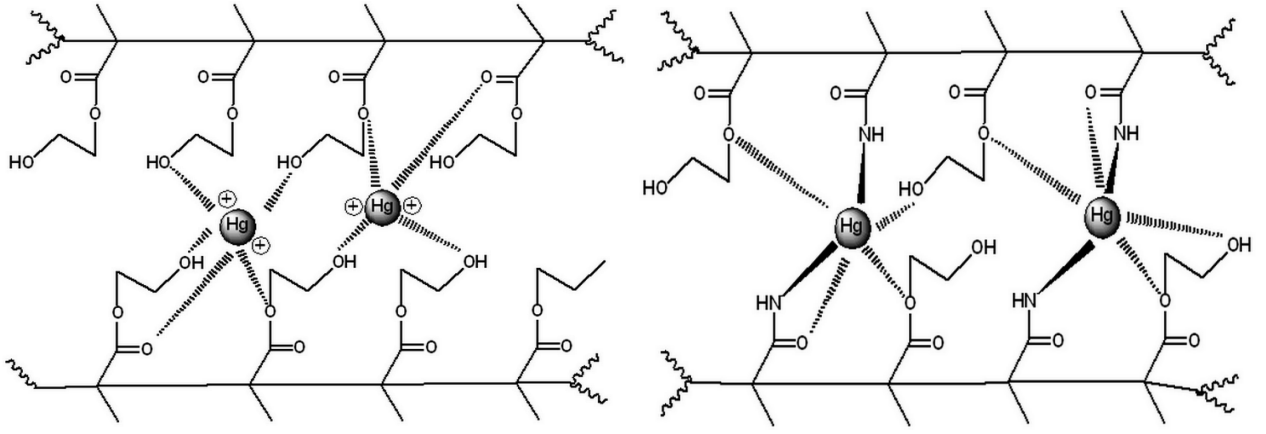

Fig. 4. The plausible interactions between the mercury(II) ions and HM hydrogel (a) or HM/ACR hydrogel (b); solid lines designate chemical interactions, dashed lines designate physical interactions

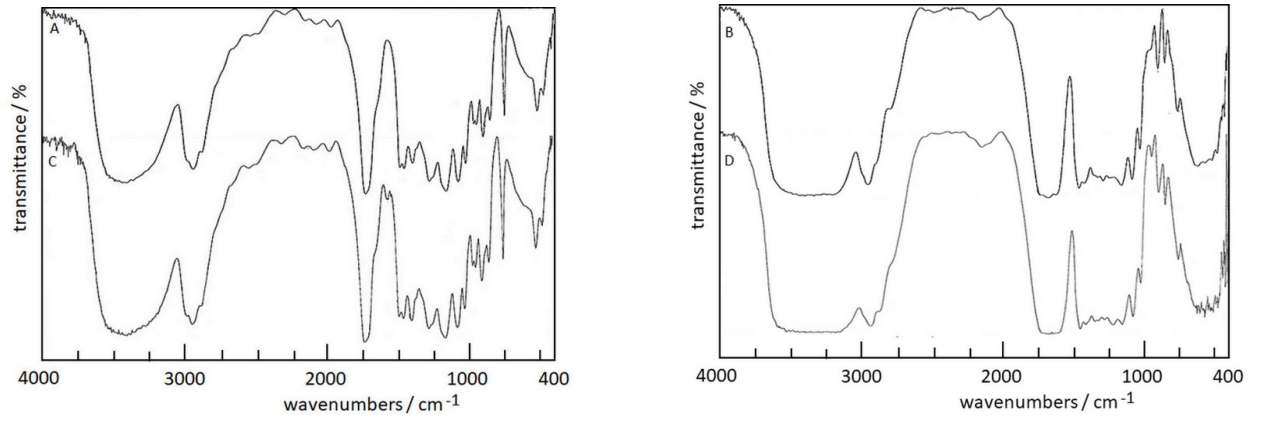

Fig. 5. FTIR spectra of the hydrogels: HM (A); Hg^{2+}−loaded HM (C); HM/ACR (B) and Hg^{2+}−loaded HM/ACR (D)

The main interaction sites of the Hg^{2+} are the N and O atoms containing several lone electron pairs on the main chains.[10] Functional groups such as –NH– (or –N=/−NH_2) and –C=O are more likely to act as binding sites in their interactions with Hg^{2+}. This is due to the fact that the soft acid of the Hg^{2+}offers high affinity to the soft bases of the –C=O groups and to the medium soft bases of the –NH–, –N=, and –NH_2 groups. Besides, O–H bonds will be another binding site by generating charge transfer between the electron-rich HM and electron-poor Hg^{2+}.[10]

The reaction appears to be general for compounds containing amide groups. Polymers/gels containing amides in their chemical structure can be considered as a suitable adsorbent in the binding of Hg^{2+}. Since HM and HM/ACR hydrogels contain functional groups such as amide, hydroxyl, and carbonyl, a plausible mechanism for interactions of these hydrogels with Hg^{2+} has been proposed (Fig. 4).[31]

To explain spectroscopically the binding of Hg^{2+} onto hydrogels, the FTIR spectra of Hg loaded−HM and −HM/ACR hydrogels are taken (Fig. 5).

The unloaded−HM hydrogel and Hg loaded−HM hydrogel spectra are the same. In contrast, the unloaded−HM/ACR spectrum has some differences if compared with the Hg loaded−HM/ACR hydrogel spectrum (Fig. 5). Due to the complexation of Hg^{2+} with acrylamide units in the HM/ACR hydrogel, the N–H bending, as well as asymmetric and symmetrical stretching vibration bands of N−H of the amide groups shifted towards the lower region, while the stretching vibration band of C=O in the amide group shifted towards the higher region (Fig. 5).

In the FTIR spectrum of HM/ACR hydrogel, C=O stretching vibrations and N−H bending of amide are observed at 1660 and 1626 cm^{-1}, respectively. Apart from these bands, C–H stretching at 2953 cm^{-1} is also observed. In the case of Hg^{2+}–HM/ACR complex, the −C=O stretching vibrations shift from 1677 to 1660 cm^{-1}, *i.e.* towards the higher region. In Hg^{2+}–HM/ACR, N−H bending stretching and N−H plane bending coupled with C–N stretching shifted towards the lower region, *i.e.* from 1626 to 1600 cm^{-1} and from 1294 to 1243 cm^{-1}, respectively.[34]

Characteristic infrared absorption bonds of the HM/ACR hydrogel linkages at the amide I (1600−1700 cm^{-1}; C=O stretch weakly coupled with C–N stretch and N–H bending), amide II (1500−1600 cm^{-1}; C–N stretching strongly coupled with N–H bending) and amide III (1200−1350 cm^{-1}; N–H plane bending coupled with C−N stretching) regions correspond to the amide structure.[35] The vibration shifting in the hydrogels may be caused by the binding of Hg^{2+} to the amide groups of polymer chains in the HM/ACR hydrogel.

The plausible binding pattern of the Hg^{2+}–hydrogel systems proposed in Fig. 4 is supported by the IR spectra.

3.4.2. Binding characterization

C_0, which is the total solute concentration in the adsorption equilibrium, is calculated according to (7):

$$C_0 = C_b + C \tag{7}$$

where C_b is the equilibrium concentration of the solutions on the adsorbent per liter solution (*bound solute concentration*); C is the equilibrium concentration of the solute in the solution (*free solute concentration*). The value of the bound concentration can be calculated by using the difference of C_0–C. For a fixed free solute concentration, C_b is proportional to the polymer concentration on the binding system; therefore, the amount bound can be conveniently expressed as the binding ratio:

$$r = \frac{C_b}{P} \tag{8}$$

Thus, with C_b in mol·L^{-1}, and P is base mol (moles of monomer units) per liter the solute represents the average number of molecules of solute bound to each monomer unit at that free solute concentration.[34]

Adsorption kinetics and equilibria are two critical physicochemical properties for evaluating the sorption process as a unit process.[37,38]

3.4.2.1. Kinetics of the mercury uptake

For metal sorption on the hydrogel surface, PFO, PSO kinetic models, and intraparticle diffusion (IPD) model are used.[39]

PFO model, which can be applied when the sorption rate of metal ions is proportional to the number of vacant sites onto the hydrogel, is shown by the following equation.

$$r = r_{\max}(1 - e^{k_1 t}) \tag{9}$$

where $r_{\max}$ and r are the amount of metal sorbed (mmol·mol^{-1}) on the hydrogels at equilibrium and at any time t; k_1 is the PFO rate constant, min^{-1}.

The PSO model is applied when the metal sorption rate is proportional to the square of the number of vacant sites on hydrogels, and its equation can be written as following:

$$r = \frac{r_{\max}^2 k_2 t}{1 + r_{\max} k_2} \tag{10}$$

where k_2 is the PSO rate constant, mol^{-1} mmol min^{-1}; r_{max} and r are as defined above.

IDF model is used to explain the role of diffusion in the sorption process. The graph between r and $t^{0.5}$ transmits the necessary information. The graph usually shows three linear regions that reflect the external mass transfer, particle diffusion, and saturation of the process.[37] IDF model equation is as following:

$$r = k_i \sqrt{t} + W \tag{11}$$

where k_i is IDF rate constant, mmol mol^{-1} $min^{-1/2}$; W is intercepted for any trial.

To investigate the sorption kinetics, the *r versus* $t^{0.5}$ is plotted for the binding kinetics of Hg^{2+} onto HM and HM/ACR hydrogels, illustrated by experimental data filled and empty circles (Fig. 6).

Binding of Hg^{2+} was increased sharply at a short contact time and gradually slowed down with the approaching equilibrium (Fig. 6). This behavior indicates the saturation of relatively available fewer adsorption sites. Its kinetic curves are smooth and continuous, and have reached saturation, indicating that monolayer Hg^{2+} is the coverage of the hydrogels (chemosphere).

To apply the PFO and PSO kinetic models to the experimental data in Fig. 6, the nonlinear regression curves indicated by solid and dashed lines are drawn, kinetic parameters and correlation coefficients (R^2) are calculated from these curves and given in Table 3.

When the values of R^2 are analyzed in Table 3, the PSO kinetics model values are closer to unity than that of the PFO kinetic model. Therefore, the suitable model for hydrogel–Hg^{2+} adsorption systems is the PSO model. Also, as seen in Table 3, Hg^{2+} was adsorbed in the HM/ACR hydrogel in greater quantity (1.65 times) and faster (4.46 times) than the HM hydrogel.

For the application of IPD model, *r vs.* $t^{0,5}$ graphs are plotted (Fig. 7). Fig. 7 shows three different regions for both HM and HM/ACR hydrogels. The first region is the external mass transfer (EMT) region with a time interval of 0–60 min, the second zone is the intraparticle diffusion (IPD) region in the 60−240 minute range, and the last zone is the saturation (SA) zone in the range of 240−480 min. Rate constants of the regions were found from the slope of the lines in Fig. 7 and listed in Table 3 with together correlation coefficients.

The rate constants of the hydrogel−Hg^{2+} adsorption systems vary as $k_{EMT} > k_{IPD} > k_{SA}$. This indicates that the EMT process is more dominant in the system in the first 60 minutes of the binding process. Furthermore, the k_{EMT} value of the HM/ACR−Hg^{2+} adsorption system was greater than that of other, while the k_{IPD} and k_{SA} values were approximately equal. Thus, it can be said that Hg^{2+} has a faster external mass transfer to the HM/ACR hydrogel than the HM hydrogel.

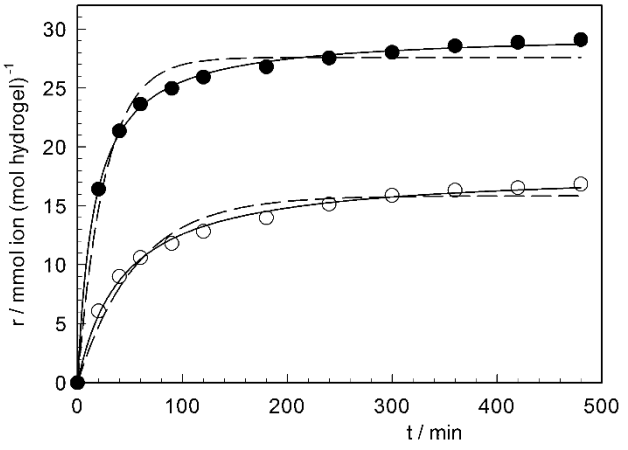

Fig. 6. The kinetic curves for the adsorption of Hg^{2+} on the hydrogels: HM (○); HM/ACR (●); PFO model fit (− − −) and PSO model fit (——)

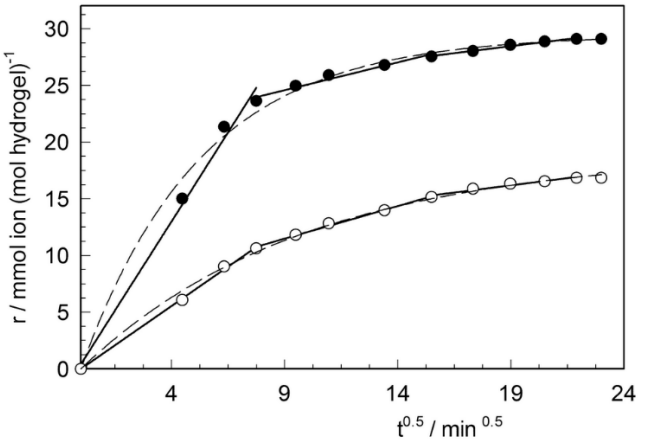

Fig 7. The intraparticle kinetic curves for the mercury(II) ions−hydrogel system: HM (○); HM/ACR (●); model fit (− − −)

Table 3. Adsorption kinetics parameters of the hydrogels

Parameter	Hydrogel	
	HM	HM/ACR
Experimental		
Equilibrium adsorption r_e, mmol mol^{-1}	16.8369	29.0960
Pseudo-first order		
Maximum adsorption r_{max}, mmol mol^{-1}	15.8469	27.5908
Rate constant k_1, min^{-1}	0.0178	0.0381
Correlation coefficient R^2	0.9709	0.9801
Pseudo-second order		
Initial r_0 or $(dr/dt)_0$, mmol mol^{-1} min^{-1}	0.4088	1.8225
Maximum adsorption r_{max}, mmol mol^{-1}	17.9783	29.6015
Rate constant k_2, mol^{-1} mol min^{-1}	1.2647	2.0833
Correlation coefficient R^2	0.9916	0.9981
Intraparticular diffusion		
External mass transfer rate constant k_{i1}, mmol mol^{-1} $min^{-1/2}$	1.3863	3.1456
Intra-particle diffusion rate constant k_{i2}, mmol mol^{-1} $min^{-1/2}$	0.5754	0.4903
Saturation rate constant k_{i3}, mmol mol^{-1} $min^{-1/2}$	0.2545	0.2474
Correlation coefficient R_{i1}^2	0.9986	0.9915
Correlation coefficient R_{i2}^2	0.9936	0.9666
Correlation coefficient R_{i3}^2	0.9640	0.9860

3.4.2.2. Influence of Hg^{2+} concentration

To determine the sorption of Hg^{2+} on HM and HM/ACR hydrogels, the graph of the *r*–*C* is plotted, and presented in Fig. 8.

The Freundlich equation is:[41,42]

$$r = k_F C^{\frac{1}{n_F}} \tag{12}$$

where r and C were predefined; k_F is the Freundlich constant; n_F is an indicator of the deviation of the binding isotherm from linearity. The n_F values are related to the Giles classification, S-, L-, and C-type isotherm. $n_F > 1$ corresponds to L-type, $n_F = 1$ to C-type and $n_F < 1$ to S-shape.[42,43] The high k_F value indicates easy uptake of the solute from the solution. Freundlich parameters are calculated from the nonlinear regression of the plots in Fig. 8, and were given in Table 4.

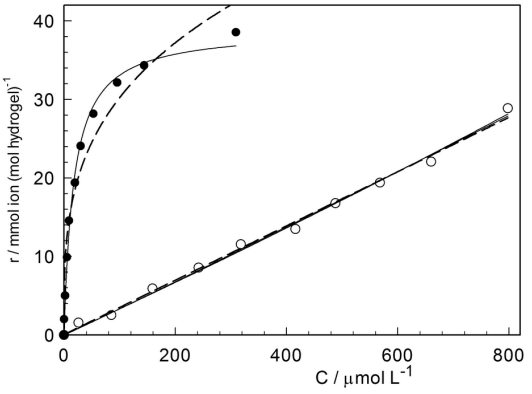

Fig 8. The binding isotherms of Hg^{2+} −hydrogel system: HM (○); HM/ACR (●); Freundlich model (− − −) and Langmuir model (——)

The n_F values for HM and HM/ACR hydrogels were found to be 1.00 to 3.33, respectively. According to these n_F values, the binding of Hg^{2+} onto HM and HM/ACR hydrogel is C-type (*Henry type*) and L-type (*Langmuirian type*), respectively.[44]

A C-type isotherm curve is a linear form, indicating that the binding ratio increases linearly with the free concentration. The L-type isotherm curve is in a plateau form and has a concave shape.[45] Initially, since most of the sorbent material absorption sites are unoccupied, there is a steep increase in binding rate with an increased free concentration in the outer solution.

On the other hand, since adsorption was determined as C-type and L-type, adsorption parameters were determined by using Henry and Langmuir's equation given below.

Henry's equation $$r = K_H C \tag{13}$$

Langmuir's equation $$r = \frac{n_L K_L C}{1 + K_L C} \tag{14}$$

where K_H (for Henry equation) and K_L (for Langmuir equation) are the binding constant, and n_L is the site density, *i.e.*, the limiting value of r for ''monolayer" coverage.

The reciprocal of n_L is the site-size u, which may be taken to represent either the average number of monomer units occupied by the bound solute molecule or, more generally, the average spacing of solute molecules when the chain is saturated. The initial binding constant, K_i, is the initial slope of the binding isotherm, and therefore the average binding strength of a solute molecule by a single monomer unit on an occupied chain. It is equal to the product $K_L n_L$.

Table 4. Adsorption parameters

Parameter	Hydrogel	
	HM	HM/ACR
Freundlich parameters		
Adsorption capacity k_F, ((mmol mol^{-1})(L mmol^{-1})$^{1/n}$)	41.1529	0.4799
Heterogeneity factor n_F	1.0000	3.3256
Isotherm type in the Giles classification	C	L
Correlation coefficient R^2	0.9953	0.9599
Langmuir parameters		
Monolayer adsorption capacity n_L, $mmol_{Hg}$ mol_P^{-1}	390.2630	38.7281
Affinity constant K_L, L·mol^{-1}	-84.3111	56678.5110
Initial binding constant K_i	32.9035	2195.0499
Site-size u, mol hydrogel·(mol mercury(II))$^{-1}$	2.5624	25.8211
Fractional occupancy θ	0.0935	0.9915
Correlation coefficient R^2	0.9957	0.9934
Range of equilibrium parameters R_L	1.1111-1.0040	0.0140-0.2614
Type of isotherm	linear	favorable
Correlation coefficient R^2	0.9957	0.9934
Henry parameters		
Henry's adsorption constant K_H, L·mol_P^{-1}	34.5889	–
Correlation coefficient R^2	0.9951	–

The maximum fractional occupancy f_{max}, attained experimentally, was calculated from the definition of fractional occupancy:[36]

$$f_{\max} = \frac{r_{\max}}{n_L} \quad (15)$$

where r_{max} is the experimental maximum r value.

Binding parameters with correlation coefficients (R^2) were calculated from the Henry and Langmuir plots (Fig. 8) and the values are also given in Table 4.

While the affinity constant value of the HM hydrogel was found to be negative, this value of HM/ACR hydrogel was both positive and very high. Therefore, it can be said that; while the affinity of Hg^{2+} to HM hydrogel is quite low, the affinity of the Hg^{2+} to HM/ACR hydrogel is quite high.

The monolayer capacities (site-density) of HM and HM/ACR hydrogel for Hg^{2+} were found to be 390.26 and 38.73 mmol Hg(II)·(mol hydrogel)$^{-1}$, respectively. The site-density of HM/ACR is precisely ten times greater than that of HM.

The u values were calculated to be 2.56 and 25.82 mol hydrogel·(mol Hg(II))$^{-1}$ for HM and HM/ACR hydrogels, respectively. Thus, it can be said that one mole of Hg^{2+} is bound to 2.56 moles of the monomeric units of the HM hydrogel, whereas one mole of Hg^{2+} is bound to 25.82 moles of the monomeric units of the HM/ACR hydrogel.

Considering the f_{max} values, it has been observed that the active binding sites of the HM/AAm hydrogel are filled with mercury ions. In contrast, 9.35 % of the active binding sites of the HM hydrogel are filled with mercury ions. This result shows that at the end of the hydrogel–mercury binding experiments, all of the active binding sites of the HM/ACR hydrogel are occupied by Hg^{2+}.

The key features of the Langmuir isotherm are given by a separation factor or equilibrium parameter (R_L, dimensionless):[40]

$$R_L = \frac{1}{1 + K_L C_0} \quad (16)$$

where K_L is the Langmuir constant, L·mmol^{-1}. The value of R_L indicates the shape of the isotherms to be either unfavorable ($R_L > 1$), linear ($R_L = 1$), favorable ($0 < R_L < 1$) or irreversible ($R_L = 0$).

The calculated R_L values as different initial Hg^{2+} concentrations are shown in Fig. 9. R_L values in the range of 0−1 indicate that Hg^{2+} are favorable for binding in the HM/ACR hydrogel. Also, lower R_L values at higher initial Hg^{2+} concentrations showed that the adsorption was more favorable at higher concentrations. The degree of favorability is generally related to the irreversibility of the system, giving a qualitative assessment of the Hg^{2+}–HM/ACR interactions. The degrees tended toward zero (the completely ideal irreversible case) rather than unity (which represents an entirely reversible case). On the other hand, R_L value of the Hg^{2+}−HM hydrogel system from 1 to 1.11 shows that the adsorption process is linear.

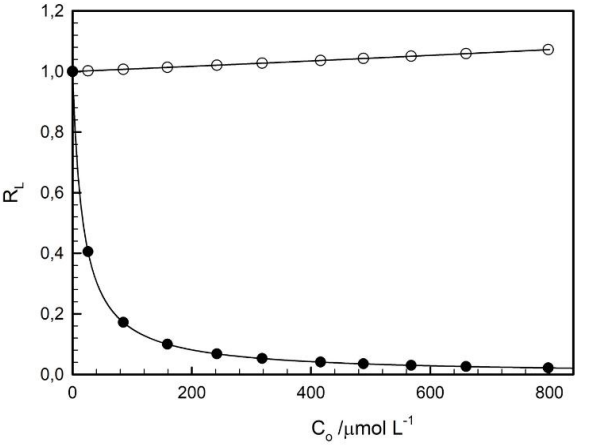

Fig. 9. Plots of separation factor *vs.* initial Hg^{2+} concentration: HM (○); HM/ACR (●)

3.4.3. The effect of ACR ratio and irradiation dose

Graphs of *r versus* ACR ratio and irradiation dose are presented in Fig. 10. The binding of Hg^{2+} onto HM and HM/ACR hydrogels was increased with an increasing ACR ratio in the hydrogel (Fig. 10a). This increase may be due to the more significant interactions between increasing amide groups and Hg^{2+}. The r value of HM/ACR hydrogel is more than three times higher than that of HM hydrogel.

The binding of Hg^{2+} in both HM and HM/ACR hydrogels was slightly reduced with the increasing irradiation dose (Fig. 10b). As the irradiation dose increases during the production of hydrogels, the crosslinking increases, and the pores to be formed become smaller. Thus, it is difficult for prominent hydrated mercury(II) ions [$Hg(H_2O)_6^{2+}$] to enter and hold in small pores.

3.4.4. The influence of temperature and adsorption thermodynamics

Since the temperature changes the binding ratio of the adsorbent, the temperature effect is an essential physico-chemical process parameter. The increase in the binding ratio with the increasing temperature indicates an endothermic process, and its decrease indicates an exothermic process. In the endothermic process, the mobility of ions and the number of active sites increase. In the exothermic process, the adsorptive forces between the ions and the active sites in the adsorbent weaken with the increasing temperature.[46]

The *r–T* plot was drawn at temperatures in the 283−323 K range. (Fig. 11). While Hg^{2+} binding was increased linearly with the increasing temperature in HM/ACR hydrogel, it decreased slowly in HM hydrogel (Fig. 11). This result shows that the binding of Hg^{2+} onto the hydrogels is the chemisorption process in HM/ACR and a physisorption process in HM.

The thermodynamic parameters of the hydrogel−Hg^{2+} sorption systems such as Gibbs free energy change (ΔG), enthalpy (ΔH) and entropy (ΔS) were calculated using the following equations:[47-49]

$$\Delta G = -RT \ln K_C \quad (17)$$

where $K_C = C_b/C$ is the distribution coefficient for sorption at a temperature and determined as:

$$\ln K_C = -\frac{\Delta H}{RT} + \frac{\Delta S}{R} \quad (18)$$

The logarithmic distribution coefficient values *versus* the inverse temperature values are plotted and presented in Fig. 12. The values of ΔG, ΔH, and ΔS were calculated using the slope and the intersection of the lines.

The values of ΔG were found as negative, and the negative values confirm the feasibility of the process and the spontaneous nature of Hg^{2+} ions. The positive value of ΔH shows the endothermic nature of the process. The order of magnitude of the ΔH value and the fact that the quantity adsorbed increased with a rise in the temperature suggested that the adsorption was of a chemical type. While the ΔH value of HM/ACR hydrogel (6.5 kJ·mol^{-1}) was quite significant, the ΔH value of HM hydrogel (0.2 kJ mol^{-1}) was close to zero. This shows that Hg^{2+} chemically binds to the HM/ACR hydrogel, and that it is bound to HM hydrogels with very weak physical bonds. The calculated positive ΔS values show the increased randomness at the hydrogel/solution interface during the sorption.

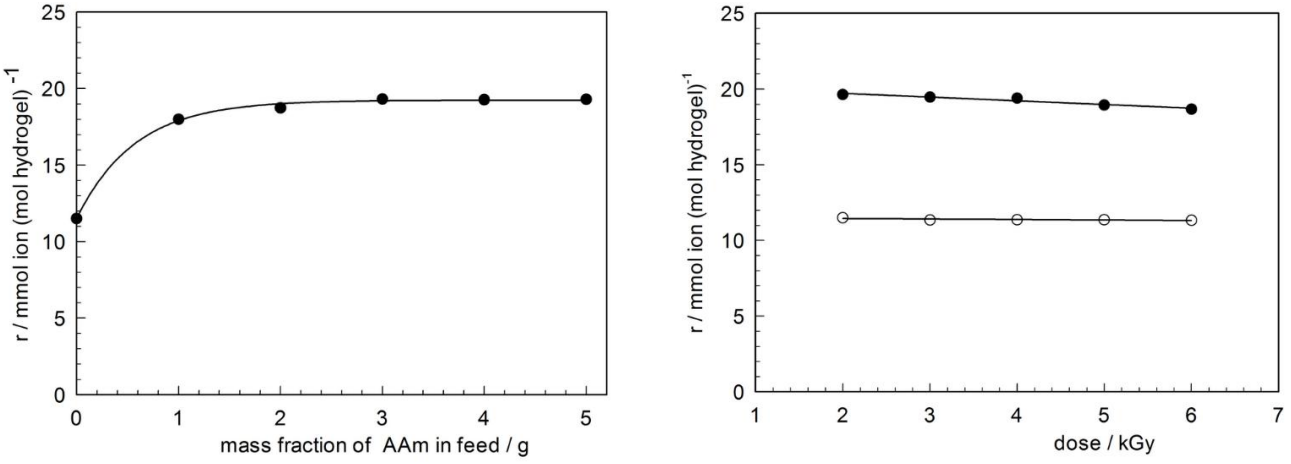

a) b)

Fig. 10. The effect of ACR content (a) and radiation dose (b)on the binding of Hg^{2+} onto the hydrogels: HM (○); HM/ACR (●)

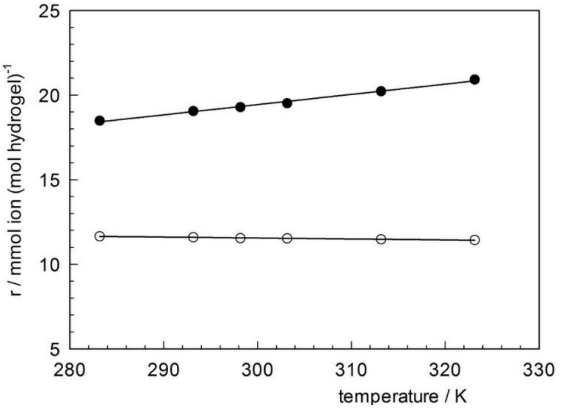

Fig. 11. The effect of temperature on the binding of Hg^{2+} onto the hydrogels: HM (○); HM/ACR (●)

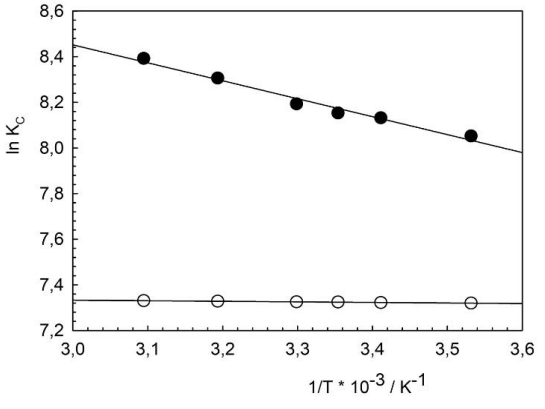

Fig. 12. Plots of lnK_C *versus* 1/*T* for adsorption of Hg^{2+} onto the hydrogels: HM (○); HM/ACR (●)

3.4.5. The effect of counter anions in the mercury salts

To examine the influence of counter anions (*i.e.,* CH_3COO^-, NO_3^-, SO_4^{2-}, or Cl^- anions) in the mercury salt solutions on the sorption of Hg^{2+} onto hydrogels, the binding ratio values were calculated and shown in Fig. 13 as a bar graph.

The binding ratio for counter ions in mercury(II) solutions are increased in the following order:

$$r_{sulfate} > r_{acetate} > r_{nitrate} > r_{chloride}$$

The binding ratio of HM/ACR hydrogels in this order is 1.3–2.2 times higher than that of HM hydrogel. Binding ratio values in salt containing chlorine ions are 3–8 times smaller than that of other counter ions. The presence of chloride ions in the solution affects the mercury sorption process. The high affinity of Hg^{2+} cations against the Cl^- anion is also well known in chemistry.[31,33] Thus, mercury ions tightly bound to chloride have the less affinity for hydrogels.

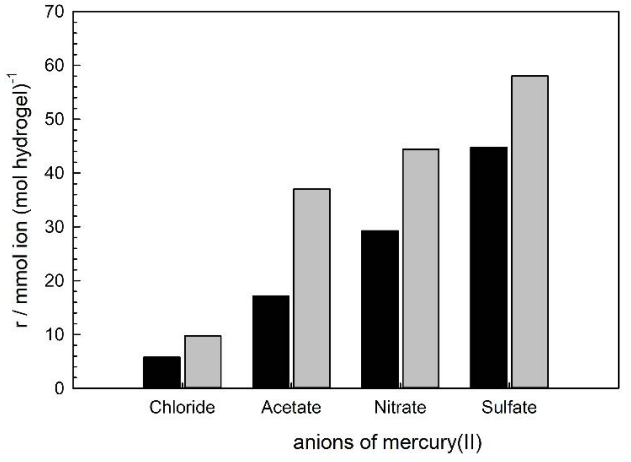

Fig 13. The influence of counter anions on mercury(II) ion uptake: HM (■); HM/ACR (□)

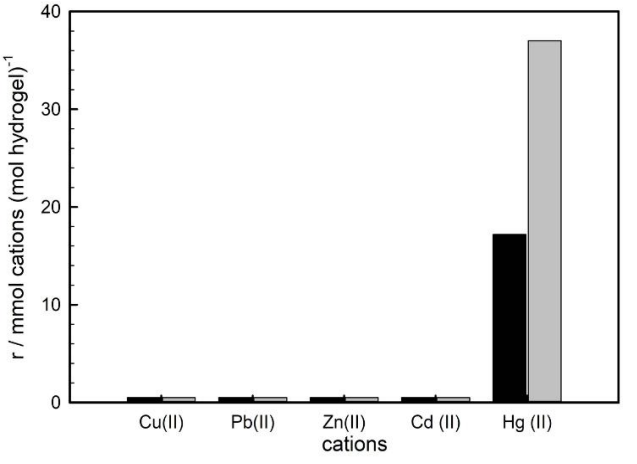

Fig 14. The binding of metal cations onto the hydrogels: HM (■); HM/ACR (□)

3.4.6. Selectivity test

Selective adsorption is of particular importance for the separation of metal ions from solutions or wastewater. Adsorption experiments for Hg^{2+} selectivity of hydrogels were carried out in the presence of potentially contaminating metal ions (Cu^{2+}, Pb^{2+}, Zn^{2+}, and Cd^{2+}). The quintet mixture solutions containing foreign metal ions and Hg^{2+} were used, and the removal of mercury and accompanying metal ions were investigated. The presence of foreign cations did not affect the sorption of mercury on HM and HM/ACR hydrogels, and the amount of Hg^{2+} ion absorbed remained almost at the same level (Fig. 14).

Since the contaminated metal ions studied do not have adsorption on hydrogels, it is seen that HM and HM/ACR hydrogels are highly selective and effective in removing mercury(II), at least in the presence of foreign cations.

3.4.7. Recovery of mercury from the hydrogels

Since mercury-amide linkages are hydrolyzed after treatment with strong acids, the use of strong acids is not suitable for desorption of Hg^{2+} absorbed. The use of hot CH_3COOH to avoid hydrolysis of amide groups is well suited for desorption of absorbed Hg^{2+}. While there is no hydrolysis reaction with hot CH_3COOH, and due to the volatility of hot CH_3COOH, it does not cause side reactions such as transamidation. Another essential advantage of CH_3COOH is that it is safe and environmentally friendly in large–scale applications.[32] In this study, it was observed that 95 % of the absorbed Hg^{2+} are desorbed for one hour by the first treatment with hot CH_3COOH.

4. Conclusions

In light of the results found, this study reveals that by incorporating the acrylamide comonomer into 2-hydroxyethyl methacrylate based polymers or hydrogels, the ability of Hg^{2+} ions to bind to these structures can be greatly increased. Such polymeric sorbents seem very promising due to their extremely high binding capacities, ion selectivity, reusability, and the easiness of handling with the safety of the environment.

References

[1] https://www.atsdr.cdc.gov/spl/index.html
[2] https://www.epa.gov/mercury/basic-information-about-mercury

[3] Amde, M.; Yin, Y.; Zhang, D.; Liu, J. Methods and Recent Advances in Speciation Analysis of Mercury Chemical Species in Environmental Samples: A Review. *Chem. Speciat. Bioavailab*. **2016**, *28*, 51-65. https://doi.org/10.1080/09542299.2016.1164019
[4] Mahbub, K.R.; Krishnan, K.; Naidu, R.; Andrews, S.; Megharaj, M. Mercury Toxicity to Terrestrial Biota. *Ecol. Indic*. **2017**, *74*, 451-462. https://doi.org/10.1016/j.ecolind.2016.12.004
[5] McNutt, M. Mercury and Health. *Science* **2013**, *341*, 1430. https://doi.org/10.1126/science.1245924
[6] de Almeida Rodrigues, P.; Ferrari, R.G.; dos Santos, L.N.; Conte-Junior, C.A. Mercury in Aquatic Fauna Contamination: A Systematic Review on its Dynamics and Potential Health Risks. *J. Environ. Sci*. **2019**, *84*, 205-218. https://doi.org/10.1016/j.jes.2019.02.018
[7] Natasha; Shahid, M.; Khalid, S.; Bibi, I.; Bundschuh, J.; Niazi, N.K.; Dumat, C. A Critical Review of Mercury Speciation, Bioavailability, Toxicity and Detoxification in Soil-Plant Environment: Ecotoxicology and Health Risk Assessment. *Sci. Total Environ*. **2020**, *711*, 134749. https://doi.org/10.1016/j.scitotenv.2019.134749
[8] Yoshino, K.; Mori, K.; Kanaya, G.; Kojima, S.; Henmi, Y.; Matsuyama, A.; Yamamoto, M. Food Sources are More İmportant than Biomagnification on Mercury Bioaccumulation in Marine Fishes. *Environ. Pollut*. **2020**, *262*, 113982. https://doi.org/10.1016/j.envpol.2020.113982
[9] Milioni, A.L.V.; Nagy, B.V.; Moura, A.L.; Zachi, E.C.; Barboni, M.T.S.; Ventura, D.F. Neurotoxic İmpact of Mercury on the Central Nervous System Evaluated by Neuropsychological Tests and on the Autonomic Nervous System Evaluated by Dynamic Pupillometry. *Neurotoxicology* **2017**, *59*, 263-269. https://doi.org/10.1016/j.neuro.2016.04.010
[10] Huang, S.; Ma, C.; Liao, Y.; Min, C.; Du, P.; Jiang, Y. Removal of Mercury(II) from Aqueous Solutions by Adsorption on Poly(1-amino-5-chloroanthraquinone) Nanofibrils: Equilibrium, Kinetics, and Mechanism Studies. *Nanomater*. **2016**, *2016*, 7245829. https://doi.org/10.1155/2016/7245829
[11] Saberi, A.; Sadeghi, M.; Alipour, E. Design of AgNPs -Base Starch/PEG-Poly (Acrylic Acid) Hydrogel for Removal of Mercury (II). *J. Polym. Environ*. **2020**, *28*, 906-917. https://doi.org/10.1007/s10924-020-01651-9
[12] Jamwal, H.S.; Ranote, S.; Kumar, D.; Chauhan, G.S.; Bansal, M. Gelatin-Based Mesoporous Hybrid Materials for Hg2+ İons Removal from Aqueous Solutions. *Sep. Purif. Technol*. **2020**, *239*, 116513. https://doi.org/10.1016/j.seppur.2020.116513
[13] Shalla, A.H.; Yaseen, Z.; Bhat, M.A.; Rangreez, T.A.; Maswal, M. Recent Review for Removal of Metal İons by Hydrogels. *Sep. Sci. Technol*. **2018**, *54*, 89-100. https://doi.org/10.1080/01496395.2018.1503307
[14] Wang, X.; Wang, A. Adsorption Characteristics of Chitosan-g-Poly(acrylic acid)/Attapulgite Hydrogel Composite for Hg(II) Ions from Aqueous Solution. *Sep. Sci. Technol*. **2010**, *45*, 2086-2094. https://doi.org/10.1080/01496395.2010.504436
[15] Khozemy, E.E.; Nasef, S.M.; Mohamed, T.M. Radiation Synthesis of Superabsorbent Hydrogel (Wheat Flour/Acrylamide) for Removal of Mercury and Lead Ions from Waste Solutions. *J. Inorg. Organomet. Polym. Mater*. **2020**, *30*, 1669-1685. https://doi.org/10.1007/s10904-019-01350-6
[16] Saraydin, D.; Yildirim, E.S.; Karadağ, E.; Güven, O. Radiation-Synthesized Acrylamide/Crotonic AcidHydrogels for Selective Mercury (II) Ion Adsorption. *Adv. Polym. Technol*. **2016**, *37*, 822. https://doi.org/10.1002/adv.21725
[17] Darwis, D.; Erizal Abbas, B.; Nurlidar, F.; Putra, D. Radiation Processing of Polymers for Medical and Pharmaceutical Applications. *Macromol. Symp*. **2015**, *353*, 15-23. https://doi.org/10.1002/masy.201550302
[18] Chmielewski, A.G.; Haji-Saeid, M.; Ahmed, S. Progress in Radiation Processing of Polymers. *Nucl. Instrum. Methods Phys. Res. B* **2005**, *236*, 44-54. https://doi.org/10.1016/j.nimb.2005.03.247
[19] Dafader, N.C.; Adnan, M.N.; Haque, M.E.; Huq, D.; Akhtar, F. Study on the Properties of Copolymer Hydrogel Obtained from Acrylamide/2-hydroxyethyl Methacrylate by the Application of Gamma Radiation. *Afr. J. Pure Appl. Chem*. **2011**, *5*, 111-118.
[20] Güven, O.; Şen, M.; Karadağ, E.; Saraydin, D. A Review on the Radiation Synthesis of Copolymeric Hydrogels for Adsorption and Separation Purposes. *Radiat. Phys. Chem*. **1999**, *56*, 381-386. https://doi.org/10.1016/s0969-806x(99)00326-6
[21] Öztop, H.N.; Öztop, A.Y.; Işikver, Y.; Saraydin, D. Immobilization of Saccharomyces Cerevisiae on to Radiation Crosslinked HEMA/AAm Hydrogels for Production of Ethyl Alcohol. *Process Biochem*. **2002**, *37*, 651-657. https://doi.org/10.1016/s0032-9592(01)00254-0
[22] Laird, F.W.; Smith, S.A. Determination of Mercury with s – Diphenylcarbazide. *Ind. Eng. Chem. Anal. Ed*. **1938**, *10*, 576-578. https://doi.org/10.1021/ac50126a002
[23] Hamdy, S.M.; El-Sigeny, S.; Abou Taleb, M.F. Immobilization of Urease on (HEMA/IA) Hydrogel Prepared by Gamma Radiation. *J. Macromol. Sci. A* **2008**, *45*, 980-987. https://doi.org/10.1080/10601320802453740
[24] Rapado, M.; Peniche, C. Synthesis and Characterization of pH and Temperature Responsive Poly(2-hydroxyethyl Methacrylate-co-acrylamide) Hydrogels. *Polímeros* **2015**, *25*, 547. https://doi.org/10.1590/0104-1428.2097
[25] Kalaivani, S.S.; Vidhyadevi, T.; Murugesan, A.; Thiruvengadaravi, K.V.; Anuradha, D.; Sivanesan, S.; Ravikumar, L. The Use of New Modified Poly(acrylamide) Chelating Resin with Pendent Benzothiazole Groups Containing Donor Atoms in the Removal of Heavy Metal İons from Aqueous Solutions. *Water Resour. Ind*. **2014**, *5*, 21-35. https://doi.org/10.1016/j.wri.2014.04.001
[26] Saraydın, D.; Işıkver, Y.; Karadağ, E. A Study on the Correlation Between Adsorption and Swelling for Poly(Hydroxamic Acid) Hydrogels-Triarylmethane Dyes Systems. *J. Polym. Environ*. **2018**, *26*, 3924-3936. https://doi.org/10.1007/s10924-018-1257-9
[27] Üzüm, Ö.B.; Çetin, G.; Kundakçı, S.; Karadag, E. Swelling and Dye Adsorption Properties of Polyelectrolyte Semi-IPNs İncluding of Acrylamide/(3-Acrylamidopropyl)trimethyl Ammonium Chloride/poly(Ethylene Glycol). *Sep. Sci. Technol*. **2020**, *55*, 3307-3319. https://doi.org/10.1080/01496395.2019.1679836
[28] Denizli, A.; Say, R.; Arica, M.Y. Dye Affinıty poly(2-Hydroxyethyl Methacrylate) Membranes for Removal of Heavy Metal Ions. *J. Macromol. Sci. A* **2000**, *37*, 343-356. https://doi.org/10.1081/ma-100101097
[29] Türkmen, D.; Öztürk, N.; Akgöl, S.; Denizli, A. High Capacity Removal of Mercury(II) İons by poly(Hydroxyethyl Methacrylate) Nanoparticles. In *Environanotechnology*; Fan, M.; Huang, C-P.; Bland, A.E.; Wang, Z.; Slimane, R.; Wright, I., Eds.: Elsevier: Amsterdam, 2010; pp 23-38. https://doi.org/10.1016/B978-0-08-054820-3.00002-2
[30] Sharma, R.K.; Chauhan, G.S. Synthesıs and Characterızatıon of Graft copolymers of 2-Hydroxyethyl Methacrylate and Some Comonomers onto Extracted Cellulose for Use ın Separatıon Technologıes. *Bioresources* **2009**, *4*, 986-1005.

[31] Sonmez, H.B.; Senkal, B.F.; Bicak, N. Poly(acrylamide) Grafts on Spherical Bead Polymers for Extremely Selective Removal of Mercuric İons from Aqueous Solutions. *J. Polym. Sci. A* **2002**, *40*, 3068-3078. https://doi.org/10.1002/pola.10392
[32] Senkal, B.F.; Yavuz, E. Ureasulfonamide Polymeric Sorbent for Selective Mercury Extraction. *Monatsh. Chem*. **2006**, *137*, 929-934. https://doi.org/10.1007/s00706-006-0494-0
[33] Zhang, X.; Hao, Y.; Wang, X.; Chen, Z.; Li, C. Competitive Adsorption of Cadmium(II) and Mercury(II) Ions from Aqueous Solutions by Activated Carbon from Xanthoceras sorbifolia Bunge Hull. *J. Chem*. **2016**, *2016*, 4326351. https://doi.org/10.1155/2016/4326351
[34] Kumar, K.; Adhikary, P.; Tungala, K.; Sonker, E.; Krishnamoorthi, S. Heavy Metals Removal by Three Arm Star Polymer Based on 2, 4, 6-Trıs Hydroxymethyl Phenol and Polyacrylamıde. *RJLBPCS* **2017**, *3*, 45-57. https://doi.org/10.26479/2017.0301.06
[35] Hayashi, T.; Mukamel, S. Two-Dimensional Vibrational Lineshapes of Amide III, II, I and A Bands in a Helical Peptide. *J. Mol. Liq*. **2008**, *141*, 149-154. https://doi.org/10.1016/j.molliq.2008.02.013
[36] Molyneux, P.; Vekavakayanondha, S. The İnteraction of Aromatic Compounds with poly(Vinylpyrrolidone) in Aqueous Solution. Part 5.–Binding İsotherms for Phenols and *O*-substituted Phenols. *J. Chem. Soc., Faraday Trans.1*, **1986**, *2*, 291-317. https://doi.org/10.1039/f19868200291
[37] Kumar, D.; Pandey, L.K.; Gaur, J.P. Metal Sorption by Algal Biomass: From Batch to Continuous System. *Algal Res*. **2016**, *18*, 95-109. https://doi.org/10.1016/j.algal.2016.05.026
[38] Ho, Y.S.; Mckay, G. Kinetic Models for the Sorption of Dye from Aqueous Solution by Wood. *Process Saf. Environ*. **1998**, *76*, 183-191. https://doi.org/10.1205/095758298529326
[39] Liu, Y.; Liu, Y.-J. Biosorption İsotherms, Kinetics and Thermodynamics. *Sep. Purif. Technol*. **2008**, *61*, 229-242. https://doi.org/10.1016/j.seppur.2007.10.002
[40] Okeola, O.F.; Odebunmi, E.O.; Ameen, O.M. Comparison of Sorption Capacity and Surface Area of Activated Carbon Prepared from Jatropha Curcas Fruit Pericarp and Seed Coat. *Bull. Chem. Soc. Ethiopia* **2012**, *26*, 171-180. https://doi.org/10.4314/bcse.v26i2.2
[41] Freundlich, H. Über die Adsorption in Lösungen. *Z. Phys. Chem*. **1907**, *57*, 385-470.
[42] Jasim Al-Hayder, L.S.; Jasim Al-Juboory, M.H. Removal Study of İmidacloprid from Aqueous Solution by Adsorption onto Polyacrylamide Cross-Linked. *J. Chem. Pharm. Res*. **2015**, *7*, 1138-1144.
[43] Pila, A.N.; Jorge, M.J.; Romero, J.M.; Jorge, N. L.; Castro, E. A. Model Isothermal Of The Equilibrium Of The Herbicide 2,4-Dichlorophenoxyacetic Acid In Watery Phase On Soil With High Contained Organic Matter. *Pinnacle Agric. Res. Manag*. **2015**, *3*, 555-558.
[44] Giles, C.H.; Smith, D.; Huitson, A. A General Treatment and Classification of the Solute Adsorption İsotherm. I. Theoretical. *J. Colloid Interface Sci*. **1974**, *47*, 755-765. https://doi.org/10.1016/0021-9797(74)90252-5
[45] Langmuir, I. The Adsorptıon of Gases on Plane Surfaces of Glass, Mıca and Platınum. *J. Am. Chem. Soc*., **1918**, *40*, 1361-1403. https://doi.org/10.1021/ja02242a004
[46] Khatoon, H.; Rai, J.P.N. Agrıcultural Waste Materıals as Bıosorbents for the Removal of Heavy Metals and Synthetıc Dyes–A Revıew. *Oct. Jour. Env. Res*. **2016**, *4*, 208-229.
[47] García, E.R.; Medina, R.L.; Lozano, M.M.; Hernández Pérez, I.; Valero, M.J.; Franco, A.M.M.Adsorption of Azo-Dye Orange II from Aqueous Solutions Using a Metal-Organic Framework Material: Iron- Benzenetricarboxylate. *Materials* **2014**, *7*, 8037-8057. https://doi.org/10.3390/ma7128037
[48] Zhou, X.; Zhou, X. The Unıt Problem ın the Thermodynamıc Calculatıon of Adsorptıon Usıng The Langmuır Equatıon. *Chem. Eng. Commun*. **2014**, *201*, 1459-1467. https://doi.org/10.1080/00986445.2013.818541
[49] Lima, E.C.; Hosseini-Bandegharaei, A.; Moreno-Piraján, J.C.; Anastopoulos, I. A Critical Review of the Estimation of the Thermodynamic Parameters on Adsorption Equilibria. Wrong Use of Equilibrium Constant in the Van't Hoof Equation for Calculation of Thermodynamic Parameters of Adsorption. *J. Mol. Liq*. **2019**, *273*, 425-434. https://doi.org/10.1016/j.molliq.2018.10.048

Received: June 19, 2020 / Revised: July 09, 2020 / Accepted: October 22, 2020

СЕЛЕКТИВНЕ ВИДАЛЕННЯ РТУТІ(II) З ВИКОРИСТАННЯМ ГІДРОГЕЛІВ, ПРИГОТОВЛЕНИХ ЗА ДОПОМОГОЮ ГАММА-ВИПРОМІНЮВАННЯ

Анотація. *Для селективного видалення ртуті(II) із використанням випромінювання синтезували гідрогелі 2-гідроксиетилметакрилат (HM) та 2-гідроксиетилметакрилат/акриламід (HM/ACR). Проведено дослідження гідрогелів в процесах набухання, дифузії та зв'язування. Встановлено, що параметри набухання для системи HM/ACR-Hg^{2+} є вищими, ніж для систем HM-Hg^{2+}. Визначено, що зв'язування ртуті відноситься до С-типу для HM та L-типу для гідрогелів HM/ACR. Параметри зв'язування розраховували за допомогою моделей Фрейндліха, Ленгмюра та Генрі. Досліджено вплив концентрації Hg^{2+}, дози випромінювання, вмісту акриламіду, температури та протийонів. Встановлено, що зв'язування та набухання HM збільшуються із включенням акриламіду. Доведено, що гідрогелі HM/ACR поглинають лише Hg^{2+} і не поглинають йони важких металів.*

Ключові слова: *ртуть, 2-гідроксиетилметакрилат, акриламід, гідрогель, випромінювання, адсорбція.*